CERN – EUROPEAN ORGANIZATION FOR NUCLEAR RESEARCH

CLIC – Note – 1176

DC BEAM STABILITY ISSUES IN THE FIRST COMMERCIAL PROTOTYPE OF A HIGH EFFICIENCY 8MW X-BAND KLYSTRON

Igor Syratchev[1)], Zaib Un Nisa[1)], Jinchi Cai[2)], Graeme Burt[3)], Toshiro Anno[4)]
1) European Organization for Nuclear Research, Geneva, Switzerland
2) Chengdu University, China
3) Lancaster University, Lancaster, UK
4) Canon Electron Tubes & Devices Co., Ltd. (CETD), Japan

CERN-ACC-2022-0007
11/05/2022

Abstract

The first commercial prototype of the new High Efficiency (HE) 8MW klystron was built and tested at CETD in the fall of 2021. Unexpectedly, in the first tests with DC beam at different beam voltages, a number of instabilities (self-oscillations) at 21-23GHz were found. As a result, at CERN, we have launched and completed a dedicated investigation program to analyse these instabilities and developed special mitigation measures for minimization of their impact on the klystron fabrication processes. In this paper, we will report the outcome of these studies.

Geneva, Switzerland
Date: 11/05/2022

1. Introduction

The high gradient X-band testing program at CERN relies on the massive high RF power testing of different accelerating structures to establish clear limits of the structure's reliable performance. These tests are conducted in two test stations, called XBOX2 and XBOX3 [1]. XBOX3 is equipped with a pair of 6MW E37113 CETD klystrons [2] combined through a 3dB hybrid. After combination, 12 MW, 2000 ns long RF pulses go through the RF pulse compression system, so that the output compressed pulses of 50-200 ns can reach peak RF power values of 42-32MW. The peculiarity of XBOX3 is that each klystron can run at 400Hz repetition rate. With combining klystrons in pair, two test areas can be operated at 200 Hz repetition rate each by alternating the hybrid output channels using the klystron's RF phase commutation. This option is important to reduce the overall testing time, which in general needs a few 10^8 pulses per structure to complete each testing program. However, some of the accelerating structures require 20-30% higher peak RF power to reach the designed gradient. In this case the structure is moved to XBOX2, which is equipped with a single 50MW CPI VKX-8311A klystron [3], operated at 50 Hz. Clearly, such logistics brings complication in the testing program, reduces the number of available testing slots, and increases the overall testing time.

Figure 1. The first commercial prototype of the high efficiency 8MW X-band klystron.

Since 2015 intensive studies of klystron technologies were established at CERN [4]. Within this activity, a number of new alternative bunching methods were developed, that allow an increase in the klystron's RF power production efficiency by 10% to 30%, compared to existing commercial tubes at different frequencies and power levels. One such project addressed the efficiency increase in an existing 6MW E37113 CETD klystron. To minimize the fabrication cost and design efforts, it was decided to adopt a retrofit approach. In this case the nominal klystron voltage (154kV), current (94A), cathode and collector designs stay the same as in the existing klystron, and only the bunching RF circuit is modified. The original design of the high efficiency 8MW klystron achieved 60% efficiency. To reach this value

in a high perveance (1.55 μA/V$^{3/2}$) tube, COM bunching method [5] was applied. However, the length of the tube of 32cm appeared to be too excessive compared to the 13cm for the existing klystron. The next klystron evaluation was done in few sequential design steps in a collaboration between CERN and CETD. Finally, a new generic RF circuit comprising of an input cavity, five bunching cavities, single set of the 2nd harmonic coupled cavities and multi-cells output coupler provided 56% RF power production efficiency in simulations that have been benchmarked and confirmed with different computer codes at CERN and at CETD. The RF circuit length of the new tube was intentionally set to be equal to the one in the existing tube, so that the klystron's solenoid can be re-used as well. With this result, we expected the RF power to increase in the test station by 30% - from 6MW (42%) to 8MW (56%) to cover the wider range of available RF peak power for the tests in XOBX3. Another advantage of the HE version is a possibility to increase further the repetition rate, as the collector heat load is reduced. This development was supplemented with a new design of RF window provided by CERN [5], to ensure safe klystron operation at a higher power level.

The first commercial prototype of the new High efficiency (HE) 8MW klystron (see Fig.1) was built and tested at CETD in the fall of 2021. Unexpectedly, in the first tests with DC beam at different voltages, a number of instabilities (self-oscillations) at 21-23GHz were found. As a result, we have launched and completed a dedicated investigation program to analyse these instabilities and to develop mitigation measures for minimization of their impact on the klystron fabrication processes. In this paper, we will report the outcome of these studies.

2. Monotron and multipolar HE modes instabilities in the 2nd harmonic coupled cavities

During testing of the klystron in DC diode mode, a few instabilities were found when the tube voltage was gradually increased. These instabilities were measured using diode detector at the klystron output and input cavities and with spectrum analyser in the output channel. In these tests, the klystron counter coil current could be changed from 7A (nominal) up to 11A in order to change the beam radius, whilst the main coil had a fixed setting to provide a nominal strength of magnetic field of 0.4T. The first instability at a frequency of 22.5GHz was observed in the voltages range from 85kV to 125kV. The images of the signals measured at 92kV are shown in Fig. 2.

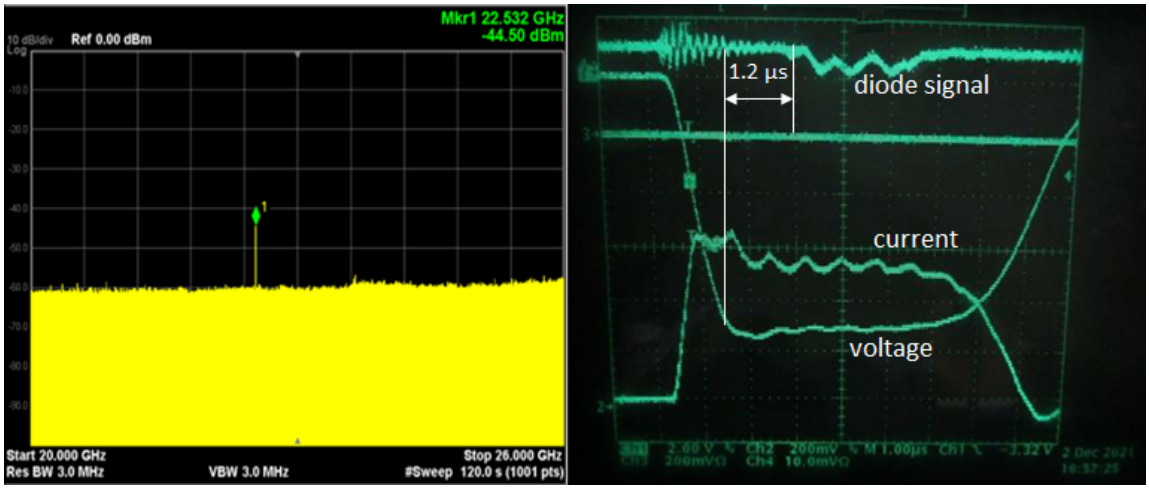

Figure 2. DC beam instability in the klystron detected at 92kV with spectrum analyser (left) and diode (right) at the klystron output.

The suspected mode responsible for this oscillation was identified as a TM_{01} π/2 mode in the 2nd harmonic cavities triplet, which has the same frequency of 22.5GHz. The wave-beam coupling mechanism in this case can be explained as a monotron oscillation. To analyse this hypothesis, we used

a CERN made klystron code KlyC [6], which has an internal module for calculation of the monotron oscillation threshold current [7]. Results of this analysis for different beam radii (beam tunnel filling factor) are summarized in Fig. 3. Following this, we can conclude that depending on the beam radius, the threshold current of monotron oscillation in the π/2 mode of the triplet can be excited within the voltage range between 70kV and 125 kV, which agrees with the experimental data. It should be noted that these results only show the threshold current, but do not have information about the oscillation onset time, which can be rather long if the threshold current value is close to the klystron current.

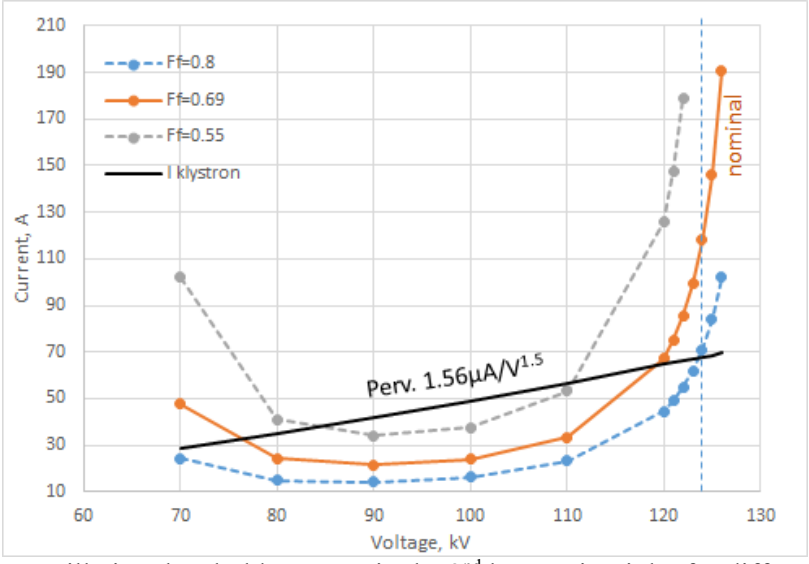

Figure 3. Monotron oscillation threshold currents in the 2nd harmonic triplet for different beam tunnel filling factors as functions of the klystron voltage.

Dedicated simulations using CST 3D PIC solver [8] were performed to crosscheck the KlyC results. These simulations confirmed the monotron oscillation hypothesis. In Fig.4, particle trajectories inside the triplet simulated at 92kV beam voltage and filling factor of 0.8, are shown. The onset time of oscillation in this simulation was around 900ns, which is in agreement with onset time indicated in Fig.1 (~1200ns), accounting for the larger beam radius that was used in simulations.

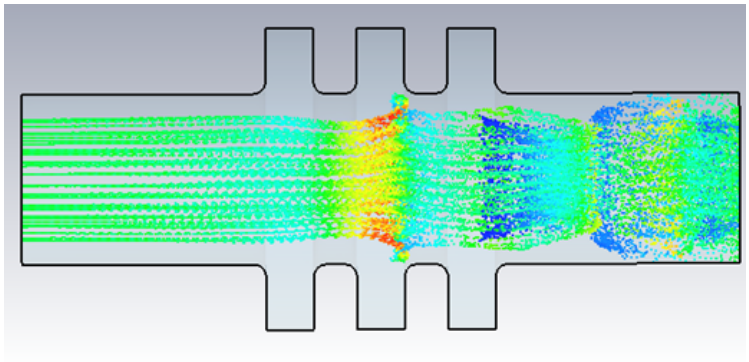

Figure 4. Particle trajectories simulated in CST 3D PIC solver at 92kV beam voltage.

The original design of the 2nd harmonic triplet was targeted for the highest effective impedance, to support a larger klystron bandwidth and to allow for relaxed fabrication tolerances. The monotron oscillations in the triplet can be mitigated by adjusting (reducing) the triplet period [7]. We have found that by reducing the iris thickness to 60% of the original value, the minimal threshold current will exceed the klystron current by at least 50% at its lowest point around 58kV. However, the same time, effective impedance of the operating π mode will lose about 30%. Thus, the triplet concept loses its

benefit and can be substituted by two coupled cavities instead, which has a similar (5% less) effective impedance. The frequency tuning of the new 2nd harmonic doublet was optimized to recover the klystron efficiency at the operation point, whilst the klystron bandwidth was practically not affected. With a doublet solution, the danger of monotron oscillation is significantly reduced, see Fig. 5. The threshold current, even for the larger beam radius (filling factor of 0.8) exceeds the klystron current with a good margin.

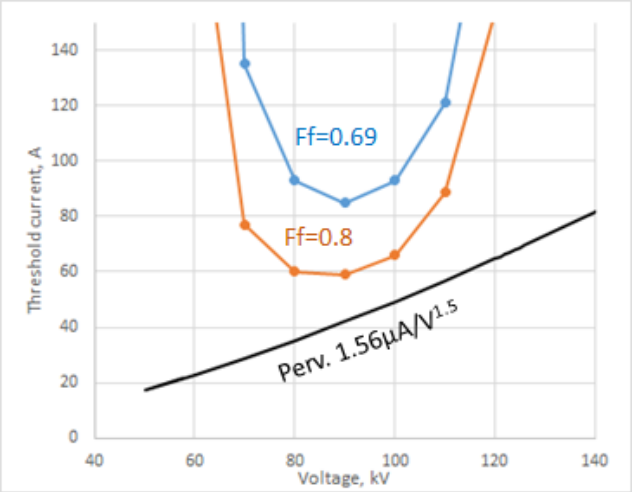

Figure 5. Monotron oscillation threshold currents in the 2nd harmonic doublet for different beam tunnel filling factors as functions of the klystron voltage

Other potential instabilities in coupled 2nd harmonic cavities are described in [9]. In this case very non-linear processes couple the beam to the spatial harmonics of the hybrid modes $HE_{N,1}$ (N=2,3), see Fig 6. These modes are at high frequencies (36.4GHz and 46.6GHz), but still stay trapped, as their cut-off frequencies are below the corresponding mode cut-off frequencies of the drift tube. A particularity of the wave-beam coupling in this case is given by the fact that these modes are rotating (angularly) modes, so that the beam can also choose to couple to one of the mode's two rotation directions. These instabilities were not found in the measurements of the klystron, yet the highest voltage used in the test was limited to 135kV (see next chapter).

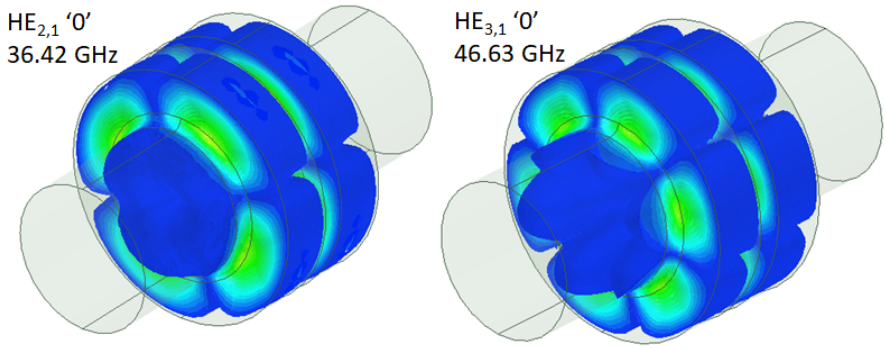

Figure 6. Electric field plots of the higher order HE modes in the 2nd harmonic doublet.

To simulate such instabilities, 3D PIC simulations are required. However, direct PIC simulations with the onset time of the instabilities unknown needs to run for long pulses (4000ns) to ensure that results can be compatible with measurements. To do these simulations we use CST 3D PIC. In this case, a single task could take up to 50 hours of physical simulation time, even when we use powerful computers with GPU accelerators. An alternative, fast and accurate method to analyse arbitrary instabilities in linear beam devices was introduced in [9]. It is based on the notation of beam-loaded quality factor (Q_{beam}), which describes the ratio of the stored energy in the given resonant mode to the

power exchange between the electron beam and the mode in a small-signal regime with a DC beam propagated through the cavity. With this method, beam dynamic calculations in PIC can be done using known (imported from CST eigensolver) eigen field-map of the mode providing a quasi steady-state regime. The mode rotation can be imposed in the simulation by using two identical orthogonal field-maps with an RF phase difference of $\pm 90^{\circ}$ between them, with the sign controlling the rotation direction. Thus, one does not need to use the full geometry in the simulation, but only the smooth beam tunnel region. To calculate the Q_{beam}, it is sufficient to measure the beam power at a collision plane for two regimes, the first without the imported mode field-map (DC) and the second with the imported mode field-map (RF). For the known intrinsic quality factor of the mode (Q_0) in the copper cavity, the condition for the instability onset will be satisfied if $Q_0/Q_{beam}<-1$. Meaning that the beam will be decelerated and extract more RF power than the RF power dissipated in the cavity walls. Such simulations were done for the new doublet design with a larger filling factor of 0.8, see Fig. 7. The simulated modes combinations showed that the klystron should be stable up to 174kV with a solenoidal field of 0.4T. The new 2nd harmonic doublet geometry was adopted for the second klystron generation. It will substitute the 2nd harmonic triplet used in the first klystron prototype.

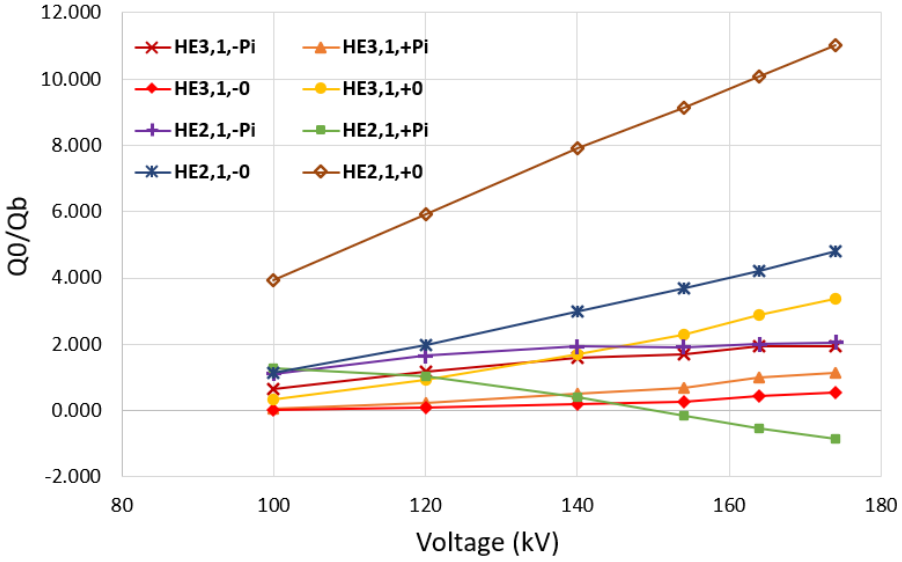

Figure 7. Q_0/Q_{beam} as a functions of beam voltage for the spatial harmonics (0 and π) of TE_{21} and TE_{31} modes. Here, + or – signs indicates the different rotation directions of the modes

3. TE_{11} coupled modes instabilities in the bunching cavities.

In the following experiments, at a voltage of 107kV, together with monotron oscillation at 22.5GHz, another oscillation was detected at 22.016GHz. With increasing voltage further up to 125kV, the monotron oscillation disappeared and oscillation at 22.016GHz was split into two lines at 21.896GHz and 21.932GHz, see Fig.8. At this voltage, the beam radius was reduced by changing the backing coil current from 7A to 11A. As a result the modes split disappeared and the only surviving mode had a frequency of 21.908GHz, see Fig 9. With 11A backing coil current, the tube was again tested at 107kV, the 22.016GHz mode was no longer seen, but the monotron oscillation at 22.5GHz was presented again. By increasing the voltage above 125kV, the 21.908GHz mode persisted, however when reaching 135kV, the ion pump on the klystron showed a pressure burst, indicating an increase in the beam interception. To avoid irreversible tube degradation, the experiments were stopped at this point for further analysis of the detected instabilities.

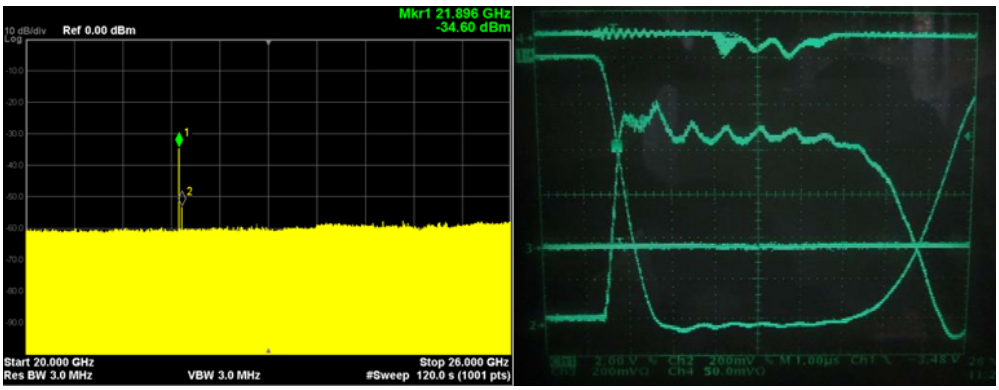

Figure 8. Dc beam instabilities in the klystron detected at 107kV with spectrum analyser (left) and diode (right) at the klystron output

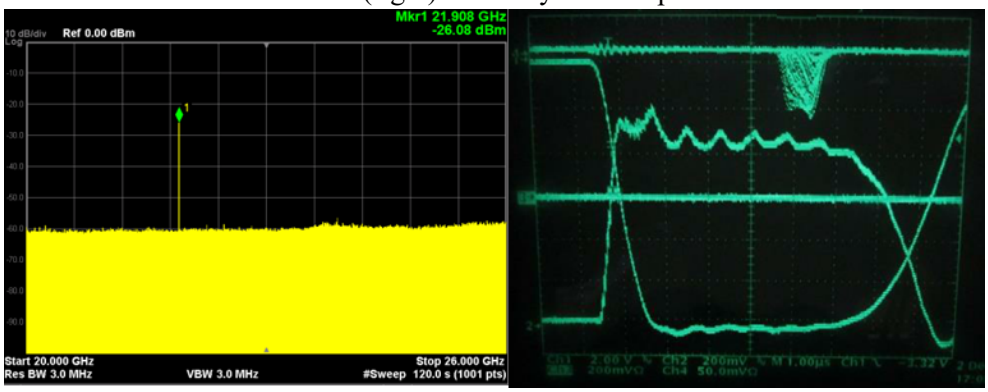

Figure 9. DC beam instability in the klystron detected at 125kV with spectrum analyser (left) and diode (right) at the klystron output

From these measurements we concluded, that apart from monotron oscillation in the triplet, there are two more modes, which are responsible for instabilities at different voltages (21.908GHz and 22.016GHz). At 125kV these two modes come into competition, which can be degenerated in a favour of the lower frequency mode by reducing the beam radius. In the original klystron design, all the bunching cavities have the same gap length, which was optimized to provide the highest impedance at the operating voltage of 154kV. Quick analysis showed a mode, which has a frequency close to 22GHz, this was a TE_{11} trapped mode in a single bunching cavity with a frequency of 22.06GHz. Furthermore, the frequency of this mode is a very weak function of the cavity outer diameter (fundamental mode tuning) and is instead governed by the gap length and beam tunnel diameter. Because more than one oscillation was found, this suggest that we have to deal with coupled TE_{11} modes. The assembly of three bunching cavities was simulated in CST eigenmode solver, see Fig. 10, and two detected modes were identified as '0' and '$\pi/2$' TE_{11} coupled modes in the bunching cavities. In the measurements, the instability at 'π' TE_{11} mode (22.31GHz) was not detected. This kind of instability is not very common. There is only one reference that we have found, which described similar effects [10].

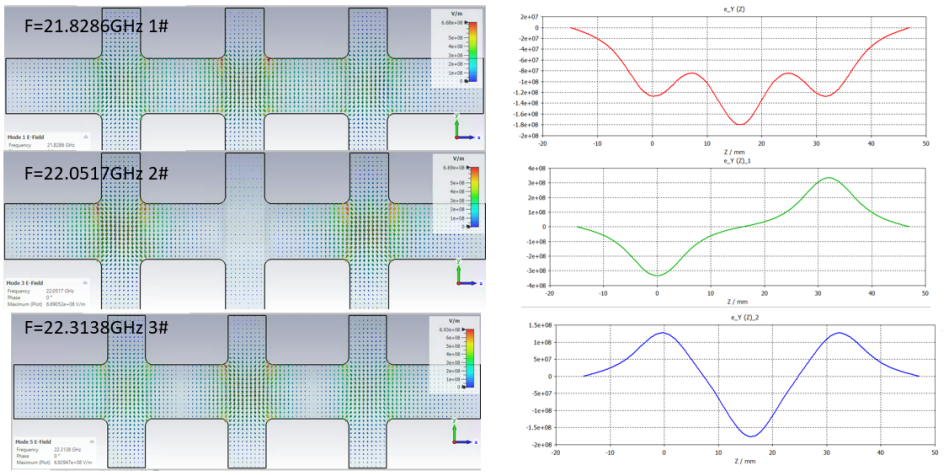

Figure 10. TE_{11} coupled modes in three bunching cavities. E filed maps are shown left and transverse component of electric filed along Z-axis are shown right.

The wave-beam coupling mechanism of these instabilities is similar to the one explained in the previous chapter for the HE modes wave-beam coupling. We used the same method to calculate the loaded beam quality and to estimate the instability regions detected in experiments. In Fig. 11, Q_0/Q_{beam} dependency on the voltage of the '0' and '$\pi/2$' TE_{11} coupled modes in three bunching cavities are shown. We used a voltage range from 107kV to 135kV in these calculations. The cases for two different beam radii were addressed, anticipating (based on measured voltage bandwidth of monotron oscillations) that with backing coil current of 7A, the beam tunnel filling factor could be around 0.8 and for 11A it could be around 0.55. At 107kV&7A, the dominant mode is the TE_{11} $\pi/2$. In the region between 120kV-125kV the '0' and '$\pi/2$' modes can compete each other, cf. Fig. 8. By reducing filling factor at 125kV&11A, the '$\pi/2$' mode disappeared, as it came close enough to the threshold of Q_0/Q_{beam} =-1. Whilst the '0' mode becomes dominant at this and higher voltages, cf. Fig. 8. With moving back to 107kV&11A there should not be any TE_{11} instabilities, as both modes are above the threshold, but monotron oscillation will rise again. These scenarios agree well with a measured data.

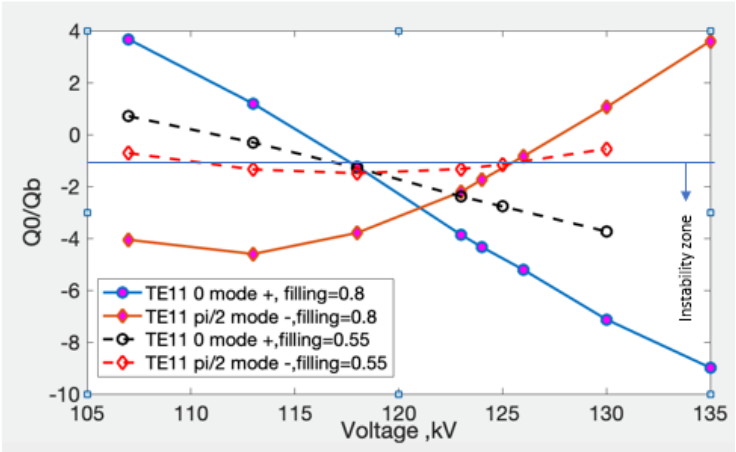

Figure 11. Q_0/Q_{beam} as a functions of beam voltage for the spatial harmonics (0 and $\pi/2$) of TE_{11} mode. Here, '+' and '-' signs indicate the different rotation directions of the modes

To mitigate the observed TE_{11} instabilities, one needs to reduce/eliminate the bunching cavities coupling. For the fixed RF circuit layout, this cannot be done by changing the distance between the cavities. The other solution is to detune TE_{11} modes frequencies in individual cavities. We have found that the only feasible solution to provide such detuning is to assign different gap length to each cavity. That will require minor changes in design (fine-tuning of the cavities fundamental modes), whilst fabrication processes and tools will not be changed.

First, we studied TE_{11} instability threshold in the individual cavities as a function of the gap length, anticipating the largest possible frequency detuning between the shortest and longest gaps. It appeared that increasing the cavity gap by 20% from its original value, there is still enough margin (factor 2) for the instability threshold at a design voltage of 154kV and filling factor of 0.8. As a compromise for the impedance, we decided that cavities gaps lengths should be varied within ± 20% interval with respect to original gap length, providing a detuning of TE_{11} modes of 1.8GHz within this range. The TE_{11} modes in the new assembly of the first three bunching cavities are shown in Fig. 12. Now one can see that modes almost look like the modes of the individual cavities, however still some residual coupling remains.

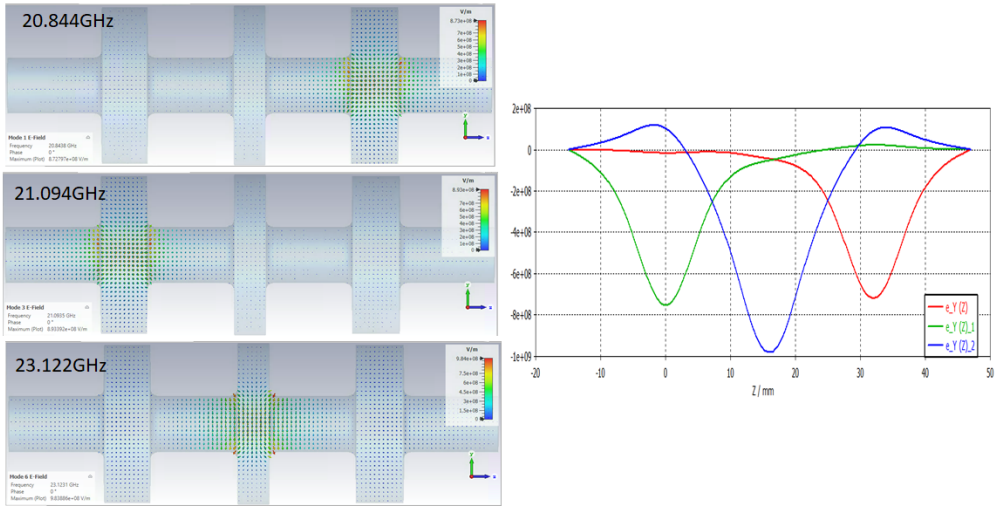

Figure 12. TE_{11} coupled modes in the new set of three bunching cavities. E filed maps are shown left and transverse component of electric filed along Z-axis are shown right

TE instabilities with the new cavities were studied for the voltage range from 100kV up to 174kV with filling a factor of 0.8 and magnetic field of 0.4T, see Fig. 13. Here one can see that modes located in cavity #2 and cavity #4 are now almost at the threshold of instability when reaching the design voltage of 154kV and the mode in the cavity #3 will not be excited, as it has positive Q_0/Q_{beam}. Such a situation still looks challenging, as simulations always have some intrinsic limits/errors that cannot be qualified prior the tests. This is why we decided to increase the safety margin by introducing some damping in the first four drift tubes. This is done using partial filling of the drift tubes with stainless steel. The amount of filling was optimized to reduce the intrinsic Q_0 factor of the TE modes by a factor of 2. Thus, safe tube operation is expect to be assured at 154kV (Q_0/Q_{beam} >-0.5 for both modes).

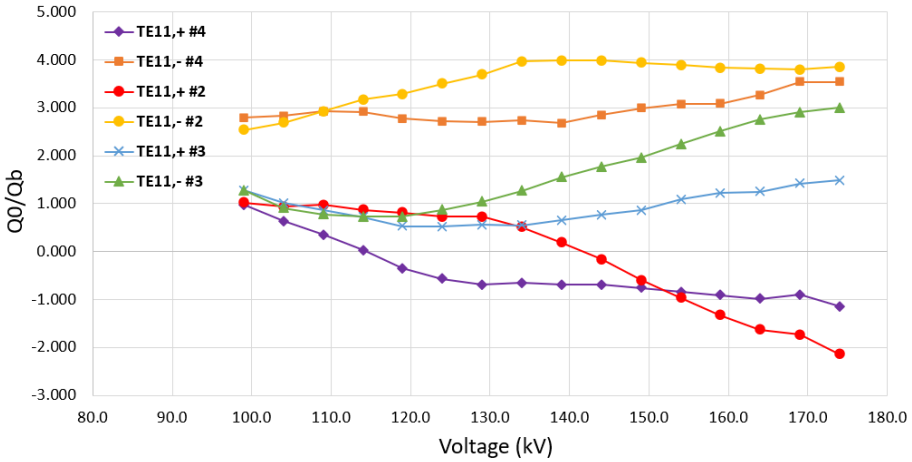

Figure 13. Q_0/Q_{beam} as functions of beam voltage for TE_{11} modes in different cavities. Here, '+' and '-' signs indicate the different rotation directions of the modes

The new klystron configuration stability was simulated using a long DC pulse PIC simulation at a design operating point of 154kV, beam tunnel filling factor of 0.69 and a magnetic field of 0.4T. In this simulation, we used the entire bunching circuit and input cavity to ensure that we had not missed any other instabilities in the rest of the bunching circuit. Particle trajectories inside the RF circuit are shown in Fig. 14. This simulation confirmed that the tube remains stable up to 4000ns.

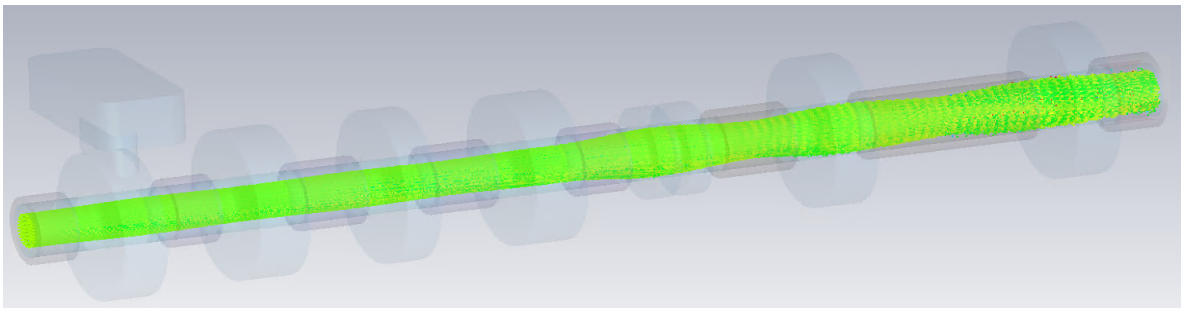

Figure 14. Particle trajectories inside the RF circuit at a design operating point of 154kV, beam tunnel filling factor of 0.69 and magnetic field of 0.4T after 4000ns simulation time.

However, the tube still could be unstable, when operated at a higher voltage than nominal. In Fig. 15, there is an example of DC beam case, when the voltage is increased up to 174kV (in attempt to reach 10MW RF output power in RF amplification regime) with a beam tunnel filling factor of 0.8 and a magnetic field of 0.4T. Clear TE mode instability is generated in the first bunching cavity. The excitation onset of this mode is 1300ns, which indicates that oscillation is close to the threshold.

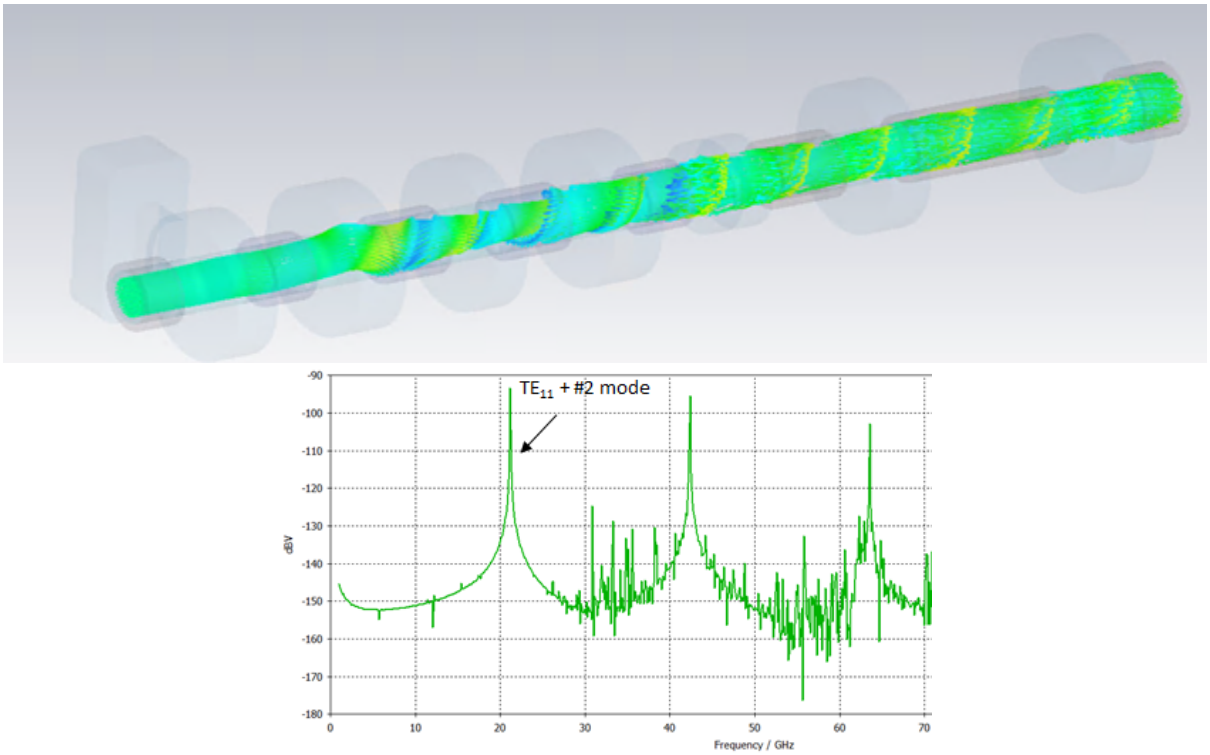

Figure 15. Particle trajectories inside the RF circuit at 174kV, beam tunnel filling factor of 0.8 and magnetic field of 0.4T after 4000ns simulation time (top) and spectrum of the signal measured by voltage monitor in the first bunching cavity (bottom).

To access higher beam voltages, the safety margin increase can be achieved using electronic measures. In Fig. 11, one can see that beam diameter has a strong impact on the instabilities threshold. In most of our simulations, we used larger filling factor of 0.8 to provide some margin. In the original klystron optics design, this value is predicted to be 0.69. In addition, it was demonstrated that if required,

the beam aperture could be reduced even further using a backing coil current. The drawback of this option will be a small power gain reduction. As an illustration, in Fig. 16 (left), Q_0/Q_{beam} values as a function of the beam tunnel filling factor are calculated for the operating voltage of 154kV and 0.4T magnetic field. The amplitude of the magnetic field also has a strong impact on the instabilities threshold. In Fig. 16 (right), one can see that at 154kV and filling factor of 0.8, by increasing the magnetic field amplitude by 5% - from 0.4T up to 0.42T, the instability threshold margin could be increased by another factor of 2. With all possible passive and active measures being used, we can expect that almost a factor of seven increase in the safety margin can be reached.

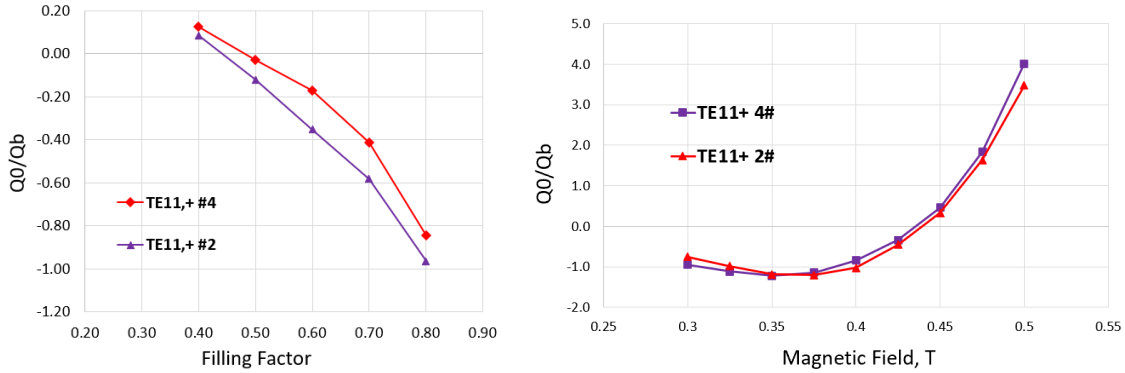

Figure 16. Q_0/Q_{beam} of two modes as functions of filling factor (154kV, 0.4T) are shown left and as functions of magnetic field (154kV, filling factor of 0.8) are shown right.

To confirm the instability mitigation efficiency using electronic measures, we simulated the case shown in Fig. 15 with a nominal beam tunnel filling factor of 0.69 and a magnetic field increased by 5% up to 0.42T, see Fig. 17. The klystron is stable after 4000ns. The last 3D PIC simulations (174kV, filling factor of 0.69 and 0.4T) were done for the assembly of the penultimate bunching cavity and output coupler, Fig. 18. No traces of instabilities were found.

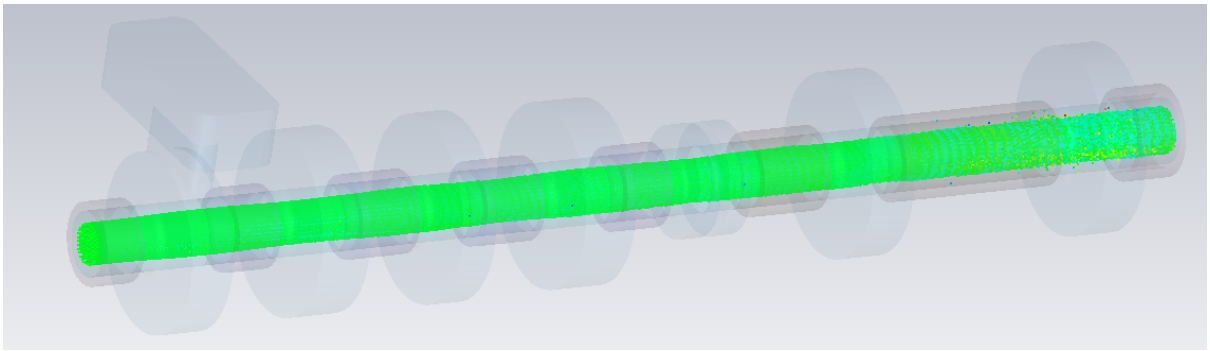

Figure 17. Particle trajectories inside the RF circuit at 174kV, beam tunnel filling factor of 0.69 and magnetic field of 0.42T after 4000ns simulation time.

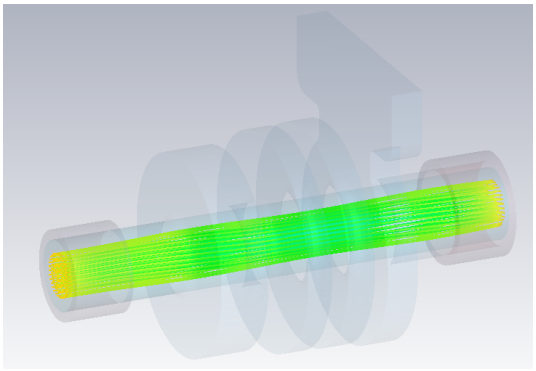

Figure 18. Particle trajectories inside the RF circuit at 174kV, beam tunnel filling factor of 0.69 and magnetic field of 0.4T after 4000ns simulation time.

The frequencies of the new cavities in the bunching RF circuit where re-tuned for the best klystron performance. In Fig. 19, snapshots of electrons trajectories at a saturated input power for the nominal operating point at 154kV (0.4T) and at 174kV (0.42T) simulated using FCI [11] computer code are shown. The average beam tunnel filling factor in these cases is 0.69. The klystron's power transfer curves are shown in Fig. 20. At 154kV saturated efficiency is 56.6%, which corresponds to 8.2MW of the output RF power. At 174kV saturated efficiency is a bit lower: 53.3%; however klystron can produce 10.5MW peak RF power at this point.

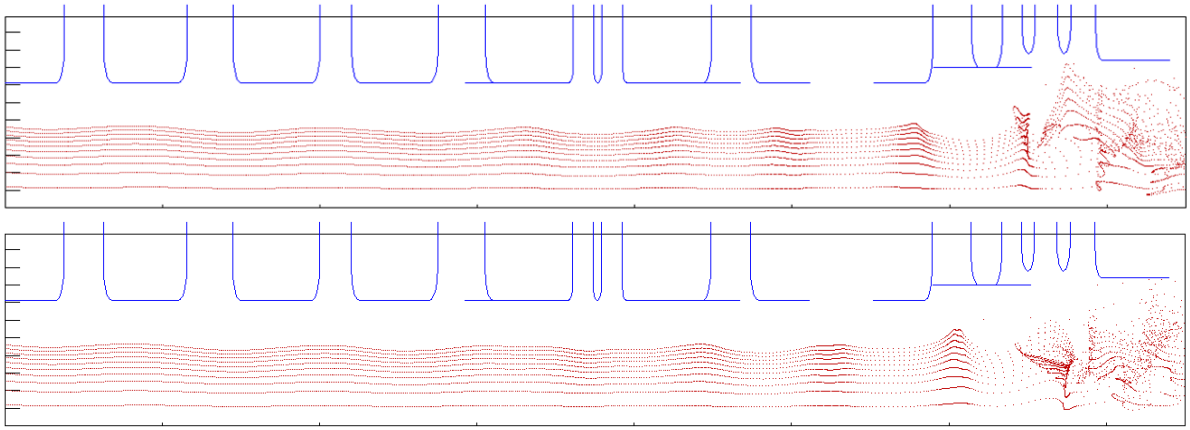

Figure 19. Snapshot of electrons trajectories at a saturated input power for the nominal operating point at 154kV, 94A and 0.4T (top); and at 174kV, 113A and 0.42T (bottom).

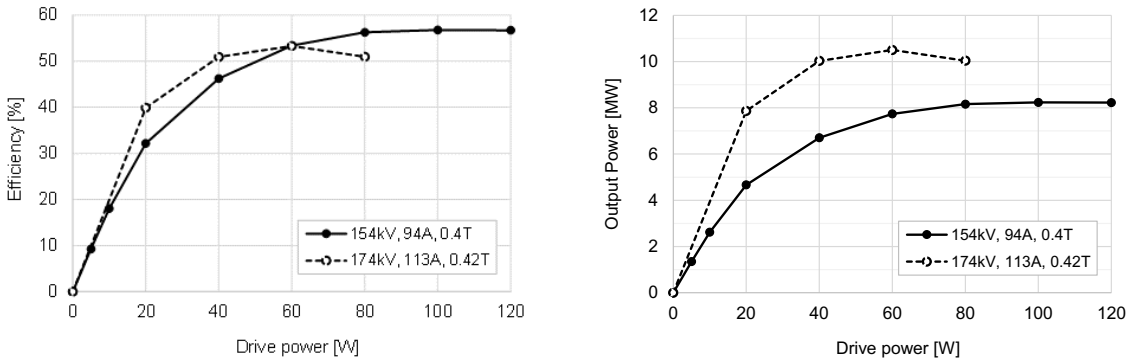

Figure 20. The klystron's power transfer curves at 154kV (0.4T) and at 174kV (0.42T).

4. Summary

The first commercial prototype of the new HE 8MW klystron was built and tested at CETD in the fall of 2021. Unexpectedly, in the first tests with DC beam at different voltages, a number of instabilities (self-oscillations) at 21-23GHz were found. An intensive investigation program to analyse these instabilities was carried out at CERN. All the instabilities sources were identified. Special passive and active mitigation measures were proposed and confirmed in full 3D PIC simulations. We expect that the modified klystron is capable to reach beam voltages as high as 174kV (above 10MW peak RF output power) and be stable. The second klystron prototype is now under fabrication at CETD and will be tested in July 2022.

References

[1] N. Catalan Lasheras et. al., 'Commissioning of XBox-3: A very high capacity X-band test stand', in Proc. of 28th Linear Accelerator Conference, East Lansing, Michigan, USA, 25 - 30 Sep 2016.
[2] Canon ETD: https://etd.canon/en/product/category/microwave/klystron.html.
[3] Communication & Power Industries (CPI): https://www.cpii.com/docs/datasheets/154/VKX-8311A%20Datasheet.pdf

[4] I. Syratchev, 'Summary of the high efficiency power source development', CLIC WS, January 2016, CERN: https://indico.cern.ch/event/449801/contributions/1945347/attachments/1215636/1775110/HEIKA_summary.pdf
[5] I. Syratchev, 'High efficiency X-band klystrons development at CERN', CLIC WS, January 2019, CERN: https://indico.cern.ch/event/753671/contributions/3272877/attachments/1783581/2902811/CLIC_WS_2018_01_Syr.pdf
[6] J.C. Cai, I. Syratchev, "KlyC: 1.5D Large Signal Simulation Code for Klystrons", IEEE Trans. on Plasma Science, vol.47, no.4, pp.1734-1741, April 2019.
[7] J.C. Cai, I. Syratchev and G. Burt, 'Accurate Modelling of Monotron Oscillations in Small- and Large-Signal Regimes' IEEE Trans. on Electron Devices, vol.67, issue.4, pp. 1797 - 1803, April 2020.
[8] CST 2018. Available at: https://www.cst.com/products.
[9] J.C. Cai, I. Syratchev and G. Burt, 'Numerical Analysis of Resonant Multipolar Instabilities in High Power Klystrons', IEEE Trans. on Electron Devices, vol.68, issue.7, pp. 3617 - 3621, June 2021.
[10] R. Kowalczyk et al., "Test of a BAC klystron," Stanford Linear Accelerator Centre, Menlo Park, CA, USA, Tech. Rep. SLAC-PUB-17102, August. 2017.
[11] T. Shintake, "High-Power Klystron Simulations using FCI-Field Charge Interaction Code", KEK Report 90-3, 1990.